PHILOSOPHICAL TRANSACTIONS OF THE ROYAL SOCIETY A
MATHEMATICAL, PHYSICAL & ENGINEERING SCIENCES

Partial Melting under Spreading Ridges [and Discussion]

Y. Bottinga, C. J. Allegre and R. N. Thompson

Phil. Trans. R. Soc. Lond. A 1978 **288**, 501-525
doi: 10.1098/rsta.1978.0031

Phil. Trans. R. Soc. Lond. A. **288**, 501–525 (1978) [501]
Printed in Great Britain

Partial melting under spreading ridges†

By Y. Bottinga‡ and C. J. Allègre
Laboratoire de Géochimie et Cosmochimie§, Institut de Physique du Globe, Université de Paris VI,
and *Département des Sciences de la Terre, Université de Paris VII, 4, Place Jussieu, Paris, France*

Factors of importance in partial melting calculations are discussed. The thermal evolution of a geochemical and petrological model of the upwelling asthenosphere beneath a ridge crest is studied numerically. Partial melting, basalt eruption and differentiation of the upwelling asthenosphere is modelled. Melt distribution and density distribution in the top 100 km of the upper mantle are calculated. Partial melting takes place in a depth interval of 25–60 km below the ridge crest. The degree of partial melting is somewhat less than 20 %. About 2.5 times more liquid is produced by partial melting in the upwelling asthenosphere than is erupted at the ridge centre. This excess liquid solidifies in the lithosphere, off-ridge axis below the Moho. The calculated results are in agreement with the observations on the oceanic ridge basalt composition, its average eruption rate, and geochemical estimates of the degree of partial melting in the sub-ridge upper mantle.

1. INTRODUCTION

The active oceanic ridge system is about 53700 km long, and has an average half spreading rate of 2.74 cm/a (Williams & Von Herzen 1974). This means that 460 m^3 of liquid magma, needed in the construction of new oceanic crust, arrives at the surface every second. In this estimate it was assumed that layer 2 and the top of layer 3 are solidified magma. It is generally accepted that this liquid is created by partial melting in the upper mantle underneath the ridge crest. In this paper general aspects of this process are discussed.

However, not only new oceanic crust is created at active spreading centres but also new oceanic lithosphere. In the axial zone of spreading ridges asthenospheric material wells up in response to the diverging motion of the plates in this region. For the purpose of this paper it is not necessary to understand the dynamics of the motion of the plates and mantle material, but the kinematics of the situation underneath the ridge crest is of great importance. During the upwelling of the asthenospheric material, partial melting occurs as a result of a diminution in pressure. The partial melt after possible modifications erupts in part at the surface to form the well known submarine pillow lavas. This is the essence of the asthenospheric upwelling model as described by Bottinga & Allègre (1973, 1976) and Bottinga (1974). In a continuing effort to understand what is happening in axial zones of spreading ridges, it was found necessary to modify the model to some extent. Certain of these modifications are described in the present contribution.

The discussion is restricted to partial melting underneath the crests of actively spreading ridges. The possible existence of plumes (Morgan 1972) and associated melting phenomena, the formation of aseismic ridges and ridge volcanoes, fall outside the scope of this paper. A knowledge of the petrology of the submarine lithosphere is of importance when partial melting

---

† Contribution I.P.G. Ns 235.
‡ Present address: Université de Nice, Parc Valrose, 06034 Nice, France.
§ Laboratoire associé au C.N.R.S. No. 196.

at spreading centres is discussed; a comprehensive review of this topic has been published by Wyllie (1971). More recent publications on this subject are by Green & Lieberman (1976) and Ringwood (1975). The asthenospheric upwelling model is a logical consequence of plate tectonics. For the latter subject the reader is referred to the book by Le Pichon, Francheteau & Bonnin (1973).

The paper is organized as follows. First the different variables of importance in the process of partial melting are reviewed (§2). In §3, the adopted model is formulated and the results calculated with this model are given. The paper is concluded with discussion of the results. In the terminology of this contribution, basalt without specification means oceanic tholeiite, also called mid-oceanic ridge basalt (m.o.r.b.). R.e.e. stands for rare-earth element.

2. Factors of importance in partial melting

To treat partial melting in the upper mantle one should know the chemical composition of this part of the Earth. Our surest sources of information on this question are kimberlites, ultramafic nodules, high temperature peridotites, the ultramafic tectonized parts of ophiolites and the seismic wave velocities (V_p and V_s) as well as the anisotropy observed for the upper mantle. The upper mantle V_p and V_s values and the submoho anisotropy found underneath the oceans (Hess 1964; Morris, Raitt & Shor 1969; Shor, Menard & Raitt 1970; Forsyth 1975; Bottinga, Steinmetz & Allègre 1976) and continents (Bamford 1973; Fuchs 1975) indicate clearly that the upper mantle is rich in olivine, or peridotitic as concluded by Forsyth & Press (1971). This evidence is in harmony with theories one has on the origin of basalt (see O'Hara 1968; Ito & Kennedy 1968; Green & Ringwood 1967) and with information furnished by kimberlites (O'Hara 1968), ultramafic nodules (White 1966; Jackson & Wright 1970), high temperature peridotites (Green 1964; Kornprobst 1969; Boudier 1976) and ophiolites (Moores 1969; Parrot 1967; Davies 1971; Juteau 1974).

However, none of these sources gives us precise information on the composition of the upper mantle, because it has become increasingly clear that all these rock types occurring at the surface of the Earth, but of undoubted upper mantle origin have undergone partial melting (Boudier & Nicolas 1972; Allègre, Montigny & Bottinga 1973; Montigny 1975; Kornprobst 1969; Dickey 1970; Loubet, Shimizu & Allègre 1975; Frey & Green 1974; Loubet 1976) with at least partial escape of the melt fraction. Hence the problem of the chemical composition of the upper mantle is not completely solved at the moment and our knowledge of the chemical composition of the upwelling asthenospheric material before extensive partial melting is still not precise. For the purpose of this paper, which is more concerned with the energetic aspects of partial melting than with petrological details, it is assumed that the initial composition of the upwelling asthenosphere is as given in table 1, column 1. The reasons for the selection of this composition will be discussed in §3.

It is obvious that the compositions listed in table 1 resemble each other very much, except in their K_2O contents. Probably, the K_2O content of composition 1 in table 1 is too high, but for our purpose this is unimportant. The chemical compositions listed in table 1 will, under upper mantle conditions, crystallize to 50–60% olivine (Fo 88) with in decreasing order of importance orthopyroxene, clinopyroxene and an aluminous phase: plagioclase, spinel or garnet.

An important parameter in partial melting calculations is the latent heat of fusion of the rock and how it depends on pressure, temperature and the compositions of the phases in the system. None of this information is available: for not a single rock is the latent heat of fusion known. The next step is to look at the latent heats of fusion for the different minerals in the rock and how these latent heats will depend on temperature and chemical composition along the fusion curve or loop. In table 2 are given different values of the latent heats of fusion at 1 atm† pressure of minerals which may occur in the mantle. The data of table 2 show that the available information on the melting behaviour of mantle materials is incomplete. Also is shown that the agreement between melting point slopes and calorimetric data is sometimes poor. Intuitively one may think that melting point slopes are less subject to errors than calorimetric data; this is not true as is evidenced by the rather late discovery of the incongruent melting of diopside (Kushiro 1973; Biggar & O'Hara 1969) and the disagreement for the two listed melting point gradients for albite.

Table 1. Estimations of volatile free upper mantle compositions (percentages by mass)

	1	2	3	4
SiO_2	46.5	45.1	45.2	42.9
TiO_2	0.5	0.2	0.7	0.2
Al_2O_3	4.3	4.6	3.5	5.8
Cr_2O_3	0.4	0.3	0.4	0.2
Fe_2O_3	—	0.3	0.5	0.3
FeO	7.8†	7.6	8.0	8.9
MnO	0.15	0.1	0.14	0.14
NiO	0.22	0.2	0.20	0.2
MgO	36.5	38.1	37.5	37.2
CaO	2.9	3.1	3.1	3.7
Na_2O	0.57	0.4	0.57	0.4
K_2O	0.12	0.02	0.13	0.003
P_2O_5	0.05	0.02	‡	‡

1. Estimation of the chemical composition of asthenospheric upwelling material, used for this paper (see also §3).
2. Average mantle pyrolite (Ringwood 1975).
3. Pyrolite III (Green & Ringwood 1970).
4. Carter (1970).

† All iron expressed as FeO.
‡ Not considered.

In general the difference between the heats of solution of the glassy state and the corresponding crystalline state is not directly comparable to the latent heat of fusion. This is well illustrated by the observations of Ferrier (1969). We do not know how one may dependably extrapolate the observed difference between the heats of solution of the glassy state and the corresponding crystalline state at a temperature considerably below the melting point, to a latent heat of fusion at the melting point temperature. The assertions of Bacon (1975) on this subject seem to be in conflict with the observations of Ferrier (1969).

Because of the incompleteness of, and the uncertainty in, the data given in table 2 it is not possible to obtain a valid estimation of the latent heat of fusion for melting in the mantle. For the calculations a value of 100 cal g^{-1}‡ was adopted. This value is reasonable in view of the melting behaviour of tholeiitic basalt, but may be wrong by a factor of 2. Of course the value will depend on pressure, temperature and the composition of the phase involved.

---

† 1 atm ≈ 10^5 Pa; 1 bar = 10^5 Pa.

‡ 1 cal ≈ 4.18 J.

TABLE 2. LATENT HEAT OF FUSION OF SOME ROCK FORMING MINERALS AT THE MELTING TEMPERATURE AND 1 atm PRESSURE

minerals	ΔH_{m} cal/g.	remarks
forsterite	—	no direct measurements have been reported
	128 ± 36‡	listed in Janaf (1971), deduced from phase diagram for Mg_2SiO_4–TiO_2
	210‡	calculated by Bradley (1962) from the Mg_2SiO_4–Fe_2SiO_4 phase diagram
	107‡	calculated by Adams & Cohen (1966) from binary phase diagrams
	400	calculated from melting point gradient (4.77 K $kbar^{-1}$ (Boyd & England 1963)) and $\Delta V_{\mathrm{m}} = 5.17\ cm^3\ mol^{-1}$†
fayalite	108	Orr (1953). Note that fayalite melts incongruently.
	109	calculated from melting point gradient (5.66 K $kbar^{-1}$ (Lindsley 1966)) and $\Delta V_{\mathrm{m}} = 3.53\ cm^3\ mol^{-1}$†
enstatite	—	no direct measurements have been reported. Enstatite melts incongruently
	146‡	listed in Robie & Waldbaum (1968) for clino-enstatite
	185‡	listed in Carmichael, Turner & Verhoogen (1974)
	179 ± 50‡	listed in Janaf (1971), deduced from phase diagram for $MgSiO_3$–TiO_2
	197	from melting point gradient (12.8 K kbar (Boyd & England 1963)) and $\Delta V_{\mathrm{m}} = 5.70\ cm^3\ mol^{-1}$†
wollastonite	—	no direct measurements have been reported
	140	from melting point gradient of pseudo wollastonite (3.83 K $kbar^{-1}$ (Kushiro 1964)) $\Delta V_{\mathrm{m}} = 1.44\ cm^3\ mol^{-1}$† (volume change for the transition speudo-wollastonite–wollastonite was neglected).
	80	from melting point gradient of wollastonite (6.73 K $kbar^{-1}$ (Kushiro 1964)) extrapolated to $P = 1$ atm and $T = 1445$ °C, and $\Delta V_{\mathrm{m}} = 5.78\ cm^3\ mol^{-1}$†
	56‡	listed in Robie & Waldbaum (1968) for pseudo wollastonite
	170‡	estimated by Kubaschewski, Evans & Alcock (1967) for pseudo wollastonite
	115‡	listed by Barin & Knacke (1973)
	160‡	listed in Carmichael *et al.* (1974)
diopside	142	Ferrier (1968). Note that diopside melts incongruently (Biggar & O'Hara 1969; Kushiro 1973)
	153	from melting point gradient (15.4 K $kbar^{-1}$ (Boyd & England 1963)) and $\Delta V_{\mathrm{m}} = 12.86\ cm^3\ mol^{-1}$†
	85‡	listed by Robie & Waldbaum (1968)
	102‡	listed by Kelley (1962)
anorthite	143	Ferrier (1969)
	334	from melting point gradient (3.0 K $kbar^{-1}$ (Hariya & Kennedy 1968)) and $\Delta V_{\mathrm{m}} = 6.40\ cm^3\ mol^{-1}$†
	104‡	listed by Carmichael *et al.* (1974)
	65‡	Kracek & Neuvonen (1952)
albite	—	no direct measurements are available
	52‡	Waldbaum (1968)
	49‡	Kracek & Neuvonen (1952)
	59	from melting point gradient (19 K $kbar^{-1}$ (Burnham & Davis 1974)) and $\Delta V_{\mathrm{m}} = 8.85\ cm^3\ mol^{-1}$†
	80	from melting point gradient (14 K $kbar^{-1}$ (Boyd & England 1964)) and $\Delta V_{\mathrm{m}} = 8.85\ cm^3\ mol^{-1}$†

† $\Delta H_{\mathrm{m}} = T\Delta S_{\mathrm{m}} = T_{\mathrm{m}}\,\Delta V_{\mathrm{m}}\,(\mathrm{d}P/\mathrm{d}T)_{\mathrm{m}}$. The melting point gradients $(\mathrm{d}P/\mathrm{d}T)_{\mathrm{m}}$ are from the indicated sources. The ΔV_{m} were calculated from the specific volumes of solids given in Robie & Waldbaum (1968), corrected for thermal expansion with the data compiled by Skinner (1966), and from the liquid densities calculated according to Bottinga & Weill (1970).

‡ Values are model dependent; they were derived from binary phase diagrams and solution models for the liquid and solid were used, as needed, or the values were derived from calorimetric observations of the transition crystal–glass at temperatures below 800 °C.

Phase transitions in the mantle, i.e. the transitions plagioclase peridotite to spinel peridotite and spinel peridotite to garnet peridotite, should also affect the value for the latent heat of fusion. The very limited information available for the pressure and temperature dependence of these transformations (no experimental observations have been reported at temperature less than 900 °C) and the concomitant specific volume changes for these transitions indicate that the heat effects are very minor. For the plagioclase–spinel peridotite transition at 1200 °C, $\Delta H \approx 0.3$ cal g^{-1} and for the spinel–garnet peridotite transition also at 1200 °C, $\Delta H \approx 1$ cal g^{-1}. However, for the basalt–eclogite transition the heat effect is more important at 1200 °C; $\Delta H \approx 36$ cal g^{-1}. In the partial melting calculations, reported in this contribution, the heat effects associated with the peridotite transformations were neglected, but for the eclogite–basalt, it was taken into account for reasons of internal consistency.

The volatile content of the mantle is of course a parameter one should consider in the analysis of partial melting in the mantle. Information on the volatile content of the mantle may be obtained from a study of magmatic gases. The topic of magmatic gases has recently been exhaustively reviewed by Anderson (1975). For our purpose the only gases of importance are CO_2, SO_2 and H_2O. These are the most abundant magmatic gases (Anderson 1975) as well as volcanic gases (Nordlie 1971; Gerlach & Nordlie 1975; Giggenbach & Le Guern 1976).

Under normal pressure and temperature conditions in the upper mantle, magnesium carbonates are stable (Newton & Sharp 1975; Kushiro, Satake & Akimoto 1975), but in upper mantle regions affected by volcanism, CO_2 occurs as bubbles. This is shown by the observed CO_2 inclusions in olivine phenocrysts (Roedder 1965) and in ultramafic inclusions (Jackson & Wright 1970) in Hawaiian alkali basalts. The great quantity of CO_2 produced by Kilauea (Pucetti & Bueddemeier 1974) indicates also that CO_2 is a free phase in the lava. Pineau, Javoy & Bottinga (1976) have observed large CO_2 inclusions in m.o.r.b. from the mid-Atlantic ridge. These inclusions were interpreted to be present long before eruption occurred. Moreover, they interpreted the carbon isotopic compositional variations observed for different inclusions in m.o.r.b. as being caused by continuous outgassing of CO_2 from ascending lava. Judging from the large quantity of SO_2 produced by volcanoes in Central America (Stoiber & Jepsen 1973) it is clear that there the lava was supersaturated with SO_2. The disastrous consequences of the Lakagigar eruption of 1783 in Iceland as described by Thorarinson (1970) indicate without ambiguity that also oceanic basalts can be supersaturated with sulphur-containing gas. None of these observations allows us to estimate the quantity of SO_2 or CO_2 present in the region where the lava is produced by partial melting.

Moore (1970) measured the water concentration in oceanic basalts. He showed that the m.o.r.b. contain less water than would have been the case if they were water saturated at $P(H_2O) = 500$ bar (pressure at the bottom of the ocean) at eruption time. The actual water content of these basalts is thus an upper limit of their initial water content at eruption time which is about 0.4 % H_2O by mass (Moore 1970; Moore & Schilling 1973). Because of the great water solubility of basaltic lavas and the fact that hydrous minerals are usually solidus minerals it is reasonable to assume that in a region of partial melting in the upper mantle all water present will concentrate in the melt. It has been suggested that phlogopite may be a residual hydrous mantle mineral (Beswick 1976). We are unaware of experiments which have shown that this mineral can survive a partial melting event to the extent needed to produce m.o.r.b. Hence from knowing the water content in the melt we may deduce an upper limit of the water content of the region where the melt was produced. That the water in submarine basalts observed by Moore (1970) is indeed of mantle origin is shown by the $^2H/^1H$ ratio of this water which greatly resembles the $^2H/^1H$ ratio for mantle water as deduced by Craig & Lupton (1976) and Sheppard & Epstein (1970).

The conclusion that the upper mantle is very dry is in agreement with the observations by Craig, Boato & White (1956) that hydrothermal sources can at best contain only negligible quantities of so-called juvenile water. However, if it is true that basalts during their ascent from the basalt source region exsolve sparingly soluble gases such as CO_2, as suggested by the previously mentioned evidence, then the observations by Moore (1970) of the water content of deep sea basalt may not give any information on the water concentration in the basalt source region. This is because the percolating bubbles of the sparingly soluble gas may have stripped the basalt also from its dissolved water, even if the basaltic liquid was water undersaturated. Currently, too little information on this topic is available and therefore this aspect has been ignored in the following paragraphs.

It is known that water depresses the solidus of possible mantle material (Kushiro, Syono & Akimoto 1968). Roughly speaking, the extent to which the mantle solidus will be depressed depends on the water activity while the quantity of partial melt produced by heating a hydrous mantle mineral assemblage to its dry solidus temperature will strongly depend on the quantity of water present. Hence when water activity is great and the quantity of water present is relatively small, which is possible if water forms a free phase in the absence of other volatiles, the mantle solidus will be greatly depressed but not much subanhydrous partial melting will take place upon heating. As discussed before, the concentration of water in the mantle is very small while volatiles like CO_2 and a sulphur-containing gas are present in non-negligible quantities; thus the activity of water in the mantle will be small. Therefore it seems that to a first approximation and for the purpose of this paper one can ignore the presence of water in the mantle.

A knowledge of the temperature–pressure path of the upwelling asthenospheric material underneath the crests of actively spreading ridges is required to calculate the amount of partial melting. In principle this may be obtained from a simultaneous solution of the three coupled partial differential equations for the conservation of the mass, momentum and energy for flow in the mantle. However, the practical difficulties in solving these equations simultaneously under realistic conditions are great; see for example De Bremaecker (1975), Richter (1973) or Turcotte & Oxburgh (1972). Because the thermal conductivity of solid silicates is rather small, the quantity of energy transported by conduction will be usually insignificant when compared with the quantity of energy transported by mass transfer in the mantle. This has a practical consequence that for single phase convection the vertical temperature variation will be given by the adiabatic gradient

$$(\partial T/\partial z)_s = g\alpha T/C_p, \tag{1}$$

where g is the gravitational acceleration, α the coefficient of thermal expansion, C_p the specific heat at constant pressure and T the absolute temperature. For asthenospheric conditions the adiabatic gradient varies from 0.3 to 0.5 °C/km which is considerably smaller than the anhydrous solidus temperature gradient for a peridotitic upper mantle, which is about 4 °C/kbar. For more detailed discussion on the use of equation 1 in the present context we refer the reader to Lang (1972). Hence if the uprising asthenospheric material is initially at a temperature not too far below its anhydrous solidus temperature, it will undergo significant partial melting if its P–T trajectory is adiabatic. The efficiency of solid state heat conduction does not only depend on the thermal conductivity but also on the local temperature gradient which depends on the distribution of thermal sinks. For the case we are discussing the thermal sinks are located at the lateral edges of the upwelling flow and at the ocean–crust interface. The analytical determination of when the adiabatic approximation for the temperature variation in vertical flowing single phase material underneath the ridge axis breaks down is impossible. Numerical

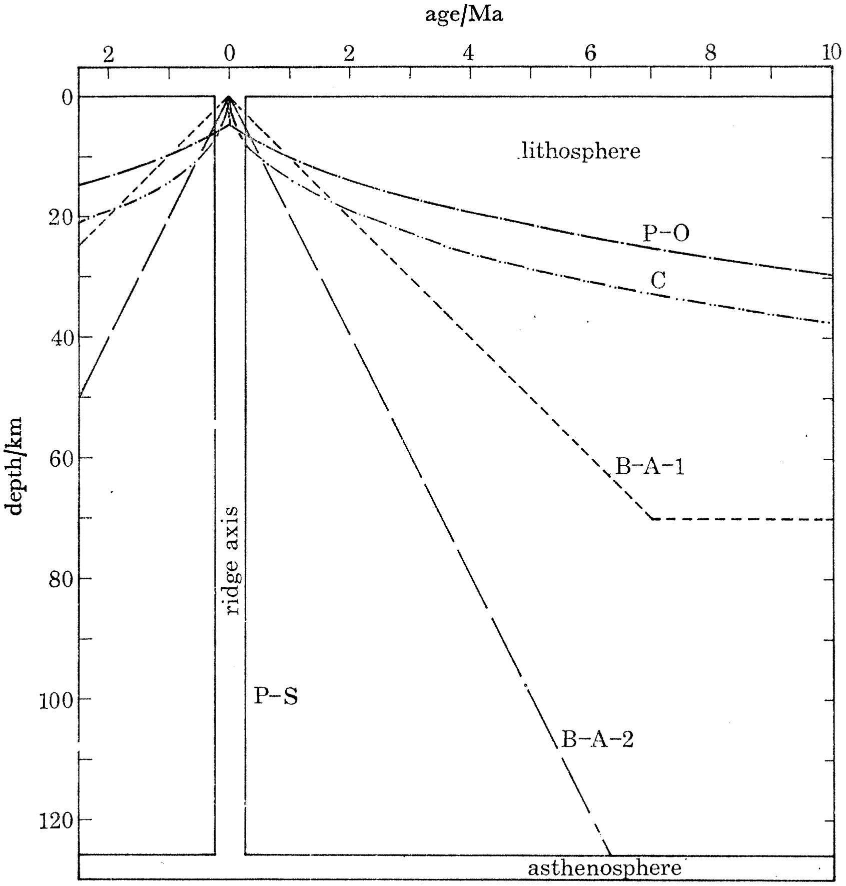

Figure 1. Shape of the lower boundary of the upper mantle region where the flow is essentially horizontal: P–O, Parker & Oldenburg (1973) and Oldenburg (1975) model; C, Crough (1975) model; B-A-1, Bottinga & Allègre (1973, 1976), Bottinga (1974) (this model was proposed originally by Langseth *et al.* (1966)); B-A-2, this work; P–S, Parsons & Sclater (1977). The width of the dike crossing the lithosphere in the axial zone has not been specified; arbitrarily it has been given a width of 5 km for this diagram. Similar models have been used by McKenzie (1967) and Sclater & Francheteau (1970).

experiments (Bottinga 1974) have shown that when the vertical velocity in the upwelling material underneath the ridge axis at depth of about 55 km or less, becomes smaller than 1 cm/a, the amount of heat transported by solid state conduction becomes non-negligible as compared to the amount of heat transported by mass transfer, i.e. the adiabatic approximation starts to become less satisfactory. Under such conditions estimates of the degree of partial melting, based on an adiabatic temperature variation, will be too high.

It is important to know whether or not the upwelling mantle material forms an open or closed system when partial melting occurs, i.e. that upon formation, melt can escape or not. The degree of partial melting due to a given amount of pressure decrease will be greater for a closed system than for an open system. This is due to the fact that when melting starts the system will leave its initial $P-T$ path, to follow a $P-T$ path given by the partial melting curve on the phase diagram for the upper mantle material. This latter $P-T$ path shows a larger decrease in temperature for a given pressure interval than the former because of the energy consuming melting process. In the closed system the melted material is constrained to have the same temperature as the solid, while in the open system the escaping melt will follow just after escape a $P-T$ path resembling the initial $P-T$ path of the solid.

Natural occurrences of partly melted rock assemblages, such as may be found in high temperature peridotites (Kornprobst 1969; Dickey 1970; Loubet 1976; Boudier 1976) and ultramafic nodules (Frey & Green 1974), suggest that in nature liquid escape occurs upon partial melting. It is evident that a certain minimum amount of melted material is needed before liquid escape takes place. For a further discussion of this point we refer the reader to the papers by Sleep (1974) and Bottinga & Allègre (1976). For the calculations reported in this paper we have assumed that liquid escape takes place.

The location of partial melting below the ridge crest depends on the flow field for the upwelling asthenospheric material. This information is a part of the solution of the convection problem. In the absence of a detailed solution, educated guesses have been made of certain aspects of this flow field. In figure 1 we have summarized this information; drawn in is the lower boundary of the uppermantle region in the axial zone of the ridge where the flow is essentially horizontal, away from the ridge axial plane.

Where partial melting takes place in these models (figure 1) depends on the width over which the material from the asthenosphere rises up from a depth at which partial melting starts. Model B–A-1 was previously used by us, we abandoned it in favour of model B–A-2 because B–A-1 produces too large a heat flow for plate ages less than 30 Ma and produces too wide a partial melting zone. These effects should be noticeable in the ocean bottom topography if the plate, even close to the ridge axis, is in isostatic equilibrium. The too large heat flow for plate ages less than 30 Ma, when compared with the observations of Parsons & Sclater (1977), is also evident in models P–O by Parker & Oldenburg (1973) and Oldenburg (1975), and C by Crough (1975). The too wide partial melting zone in model B–A-1 was not observed by Bottinga & Allègre (1976) because of a trivial error without further consequences in their computer program and was not noticed by Bottinga (1974) because he did not calculate the topography. It is evident that B–A-2, outside the axial zone of the spreading centre, is the same as the Parsons & Sclater (1977) models, P–S, except for petrological details which will be discussed in another paper.

Of the models given in figure 1, only models P–S, B–A-1 and B–A-2 have partial melting and basalt production as a logical consequence. These features are supposed to be present in an *ad hoc* fashion in models P–O and C (figure 1). As already pointed out (Bottinga & Allègre 1976) the models P–O and P–S have features, not discussed by their authors, which are geophysically, geochemically or petrologically in contradiction with the observed facts, as is now also the case for model B–A-1. For these reasons we consider in what follows model B–A-2 only.

3. THERMAL-GEOCHEMICAL MODEL

To evaluate theoretically the degree of partial melting in the upwelling asthenosphere one has to solve the energy conservation equation:

$$\partial(T+FL/C_\mathrm{p})/\partial t = \nabla.[\lambda\nabla T-\{\boldsymbol{v}+F\boldsymbol{v}_\mathrm{L}+(1-F)\boldsymbol{v}_\mathrm{S}\}T-FL\;(\boldsymbol{v}+\boldsymbol{v}_\mathrm{L})/C_\mathrm{p}]+q/C_\mathrm{p}, \tag{2}$$

where T is the temperature, F the fraction of melted material, L the latent heat of fusion, λ the thermal diffusivity, $\boldsymbol{v}$ the bulk velocity, $\boldsymbol{v}_\mathrm{L}$ and $\boldsymbol{v}_\mathrm{S}$ the velocities for solid and liquid material respectively, and q is the amount of heat generated per gram of rock per second. The velocities $\boldsymbol{v}_\mathrm{L}$ and $\boldsymbol{v}_\mathrm{S}$ are measured in a frame moving with the bulk velocity. When $F = 0$, $q = 0$ and $\boldsymbol{v}_\mathrm{S} = 0$, equation 2 reduces to the well-known heat conduction equation. The term FL/C_p at the left hand side of equation 2 expresses the absorption or liberation of latent heat when a phase change occurs. The term between curly brackets at the right hand side takes care of the convective heat transport. The last term between the square brackets is needed to keep track of the convective transport of the latent heat of fusion, stored in the liquid phase.

It is assumed that the bulk velocity field is known, i.e. $\boldsymbol{v}$ is known as a function of y and z. Y is the horizontal coordinate perpendicular to the ridge axis, its origin at the ridge axis. Z is the vertical coordinate, its origin is at the top of layer 2. Equation (2) is solved for one side of a spreading ridge in two dimensions y and z. The axial plane of the ridge is supposed to be a plane of symmetry; this gives as boundary condition that for $y = 0$ the horizontal temperature gradient equals zero for all values of z. Equation (2) is solved in a region stretching from the ridge axis to 1500 km in the y direction and for $0 < z < 126$ km. At $y = 1500$ km, it is assumed that horizontal temperature gradients are zero; this is a good approximation for plate velocities less than 3 cm/a. At $z = 126$ km, the asthenosphere is assumed to be isothermal for all values of y, the temperature being 1356 °C. This temperature is obtained from a solution of

$$\frac{\partial T}{\partial t} = \frac{\partial}{\partial z}\lambda\frac{\partial T}{\partial z}+\frac{q}{C_\mathrm{p}} = 0, \tag{3}$$

which should be valid for a steady state lithosphere far away from a spreading centre.

The boundary condition at $z = 0$ is the temperature of 0 °C at the top of the oceanic layer 2. Water penetration into the marine lithosphere in the axial region of the ridge, analysed by Lister (1974) and observed by Williams, von Herzen, Sclater & Anderson (1974), Detrick, Williams, Mudie & Sclater (1974) and Jehl (1975), is assumed to occur from 0 to 12 km from the ridge axis and to lower the temperature to 400 °C at $0 \leqslant y \leqslant 12$ km and $z = 6$ km.

The bulk velocity $\boldsymbol{v}$ is taken to be vertical in the axial region as indicated in figure 1 (model B–A-2) for $z < 126$ km; for reasons of continuity the absolute value of the vertical velocity is taken as twice the value of horizontal plate velocity. $\boldsymbol{v}_\mathrm{L}$ was estimated to be 3 cm/a, as measured in the frame moving with velocity $\boldsymbol{v}$. Previously (Bottinga & Allègre 1976; Bottinga 1974) $\boldsymbol{v}_\mathrm{L}$ was estimated to be 20 cm/a with an equation given by Franck (1968) for two phase penetrative convection. The uncertainties associated with the values of the quantities which enter into the Franck equation are large enough to allow also a $\boldsymbol{v}_\mathrm{L}$ of 3 cm/a. Computer programming conditions made us prefer this latter value. Comparison of our present results with previous ones with a $\boldsymbol{v}_\mathrm{L}$ of 20 cm/a shows that as long as the liquid moves considerably faster than the solid, as measured in a static reference frame, the effects produced by this phenomenon do not depend on the exact velocity of the liquid. The variables $\boldsymbol{v}_L$ and $\boldsymbol{v}_S$ in equation (2) are related by the conservation condition

$$\rho_L F \boldsymbol{v}_L + \rho_S (1-F) \boldsymbol{v}_S = 0, \tag{4}$$

where ρ_L and ρ_S are densities of the liquid and solid material. In equation (2) the difference between ρ_L and ρ_S was ignored; this is harmless because F is never larger than 0.2. At atmospheric pressure partial melting of a peridotite will give for not too large F a liquid with a density about 20% smaller than the solid density. Because liquids are more compressible than solids, this contrast will be smaller in the upper mantle, but probably not smaller than 10%, which is the density difference between peridotite and solid basalt. Because of this relatively large density difference between the partial melt and the residual material, the low viscosity of the partial melt (Bottinga & Weill 1972) and the fact that the residual material is readily deformable at magmatic temperatures (Kohlstedt, Goetze & Durham 1976), we believe that partly melted material in the mantle will move upwards. This has as consequences that chemical segregation will occur, because the partial melt and the residual solid have different compositions, and that the temperature in the upwelling asthenosphere will never be greatly different from the local solidus in regions where partial melting takes place. This mobility of the partial melt is also evident from studies of mantle rocks outcropping at the Earth's surface (Boudier & Nicolas 1972; Montigny 1975; Kornprobst 1969; Dickey 1970; Loubet, Shimizu & Allègre 1975; Frey & Green 1974; Loubet 1976).

The radiogenic heat term in equation (2) is relatively unimportant for the present discussion; the same value as in Bottinga & Allègre (1976), 3.9×10^{-15} cal g^{-1} s^{-1} was used.

To evaluate F, i.e. to find a relation between F and temperature, one needs a petrological model. We used the same model as in Bottinga (1974) and Bottinga & Allègre (1976) except that this time we adopted a composition of the initially upwelling asthenospheric material of 85% peridotite (KA 64–15, see Ito & Kennedy 1967) and 15% basalt (NM5, see Cohen, Ito & Kennedy 1967) as given in table 1. Previously the adopted mixture was 75% peridotite and 25% basalt; this was inspired by the pyrolite model (Ringwood 1966). However, with our mantle phase diagram (Bottinga & Allègre 1976) such a composition gave too much partial melting, and seismic velocities which tended to be too low. The present choice gives a chemical composition close to other estimates for mantle material (see table 1) and its 1 atm pressure partial melting behaviour is in reasonable agreement with other observations (see figure 2).

In the petrological model used to evaluate F, mantle material is supposed to form a binary system, with as intermediate members peridotite (KA 64–16) and the basalt (NM5). X is the compositional variable, $X = 0$ standing for basalt and $X = 1$ for peridotite. Upwelling asthenospheric material before partial melting is assumed to have the composition $X = 0.85$. The known phase relations for basalt (NM5) and peridotite (KA 64–16) as described by Ito & Kennedy (1968) make it possible to construct binary phase diagrams for all pressures occurring in the top 130 km in the mantle. This model describes well the salient points of mantle petrology as far as they are needed for the type of calculations reported here (Bottinga & Allègre 1976).

It is not for reasons of simplicity that we have adopted this highly simplified binary model for the mantle. If information on the system c.m.a.s. ($CaO–MgO–Al_2O_3–SiO_2$) were more complete, that system could just as well be used in our calculations. Our programmes are not at all limited to two-dimensional systems. One can use any dimensional system as long as the information for it is reasonably complete, i.e. liquidus and solidus hypersurfaces should be known to a certain extent at pressures from 0 to 30 kbar.

In our binary model F is given by

$$\mathrm{F} = (X - X_{\mathrm{S}})/(X_{\mathrm{L}} - X_{\mathrm{S}}), \tag{5}$$

where X is the overall composition, X_{S} the composition of the solid phase in equilibrium with a liquid phase of composition X_{L}.

The basalt solidus is given by

$$T_{\mathrm{s,\,b}}(P) = 1050 + 12.50\,P, \tag{6}$$

where P is in kilobars; the basalt liquidus by

$$T_{\mathrm{l,\,b}}(P) = 1200 + 5.10\,P \text{ for } 0 \leqslant P \leqslant 10 \text{ kbar, and} \tag{7a}$$

$$T_{\mathrm{l,\,b}}(P) = 1251 + 12.30\,(P\text{–}10) \text{ for } P > 10 \text{ kbar;} \tag{7b}$$

the peridotite solidus by

$$T_{\mathrm{s,\,p}}(P) = 1080 + 11.30(P\text{–}10) \text{ for } 0 \leqslant P \leqslant 20 \text{ kbar, and} \tag{8a}$$

$$T_{\mathrm{s,\,p}}(P) = 1306 + 12.50(P\text{–}20) \text{ for } P > 20 \text{ kbar;} \tag{8b}$$

and the peridotite liquidus by

$$T_{\mathrm{l,\,p}}(P) = 1860 + 1.0\,P. \tag{9}$$

The relations in 6–9 are derived from the results reported by Ito & Kennedy (1968). If $X \leqslant 1$, the solidus temperature T_{s} is given by

$$T_{\mathrm{s}}\,(X, P) = T_{\mathrm{s,\,b}}\,(P) + [T_{\mathrm{s,\,p}}\,(P) - T_{\mathrm{s,\,b}}\,(P)]\,X, \tag{10a}$$

and for $X > 1$

$$T_{\mathrm{s}}\,(X, P) = T_{\mathrm{s,\,p}}\,(P) + [T_{\mathrm{l,\,p}}\,(P) - \mathrm{T}_{\mathrm{l,\,b}}\,(P)]\,(X\text{–}1). \tag{10b}$$

For all X the liquidus temperature is given by

$$T_{\mathrm{l}}\,(X, P) = T_{\mathrm{l,\,b}}\,(P) + [T_{\mathrm{l,\,p}}\,(P) - T_{\mathrm{l,\,b}}\,(P)]\,X. \tag{11}$$

Equations (10*a*) and (11) are linear interpolations and are justified by the results published by Ito & Kennedy (1968). Equation (10*b*) is an extrapolation.

It was mentioned in §2 that for reasons of internal consistency the heat effect associated with the basalt–eclogite phase transition was taken into account. There is great uncertainty on the exact location of the basalt–eclogite phase transition in composition–pressure–temperature space. Somewhat arbitrarily, but not in contradiction with the results as summarized by Ringwood (1975), we have assumed that the basalt–eclogite transition occurs gradually over a temperature interval of 300 °C. The upper temperature limit of this interval is given by

$$T_{\mathrm{be,\,u}}\,(P) = 300 + 55.0\,P \tag{12a}$$

and the lower limit by

$$T_{\mathrm{be,\,l}}\,(P) = 55.0\,P. \tag{12b}$$

For $T < T_{\mathrm{be,\,l}}$ eclogite is stable and for $T > T_{\mathrm{be,\,u}}$ basalt is stable. Lack of experimental results at $T <$ 1000 °C makes justification of (12*a*) and (12*b*) difficult.

Our reasons for adopting (12*a*) and (12*b*) will be discussed in a future publication. In accordance with the volume change associated with the transition and with its P–T slope, an enthalpy change of 36 cal/g was estimated for this phase change. It was assumed that this enthalpy change is temperature independent. In the calculations the latent heat of fusion was changed when a composition of $X < 1$ underwent a phase transition in a P–T region where eclogite was stable.

For the sake of completeness the thermal effects of the basalt–eclogite transition but also those of the plagioclase peridotite–garnet–spinel peridotite and spinel peridotite–garnet peridotite transitions were taken into account when equation (2) was solved numerically. Again there is some uncertainty associated with the exact location of the two peridotite phase changes. To become convinced of this, the reader should compare the results published by Green & Ringwood (1970), McGregor (1974), O'Hara, Richardson & Wilson (1971), Herzberg & Chapman (1976) and Obata (1976). Without any particular justification we have chosen the curves published by Green & Ringwood (1970) which are for the plagioclase peridotite–spinel peridotite transition

$$T_{\mathrm{pl,s,p}}(P) = -1666 + 278.0\,P \tag{13}$$

and for the spinel peridotite–garnet peridotite transition

$$T_{\mathrm{sp,g,p}}(P) = -919 + 96.8\,P. \tag{14}$$

In our calculations the thermal conductivity was taken to be constant at 7.4×10^{-3} cal s^{-1} cm^{-1} K^{-1}; this corresponds to an average value of the observations by Schatz & Simmons (1972) for mantle rocks in the temperature interval 100–1350 °C, and is in agreement with data of Kawada (1966). The specific heat varied with temperature according to the relation

$$C_{\mathrm{p}} = 0.244 + 3.62 \times 10^{-5}\,T - 7.27 \times 10^{-3}\,T^{-2}, \tag{15}$$

where C_{p} is in cal g^{-1} K^{-1}. Equation (15) is taken from Kelley (1960), who gives this relation for diopside.

The solution of equation (2) has been described by Bottinga (1974) and Bottinga & Allègre (1973). Equation (2) is too complicated to solve analytically. The occurrence of partial melting has a consequence that implicit finite difference methods cannot be used. One needs to know at a given grid point where the temperature is to be calculated, whether or not a change phase occurs, before the temperature at the next grid point can be evaluated. Therefore, the conduction part of equation (2) was treated with a simple explicit finite difference method. However, this method cannot be used for the convective terms, because the first derivatives in these terms cause instability. Hence the convective part of equation (2) was taken care of by performing translations of temperature, liquid and solid composition and melted fraction according to the chosen velocity field; an adiabatic (equation 1) correction was applied.

Temperatures were calculated at the nodes of a square grid with 6 km sides; the time step was 50 ka. Calculations were done for a plate velocity of 1 cm/a and to some extent for 3 cm/a (i.e. spreading rates of 2 and 6 cm/a). As an initial solution was taken the temperature field obtained from a solution of equation 3, with as boundary condition a heat flow of 0.87×10^{-6} cal cm^{-2} s^{-1}. This heat flow value is in agreement with the steady state heat flow, far away from the spreading centre as deduced by Parsons & Sclater (1977). The calculation was continued until the temperature at 1500 km away from the spreading centre attained a steady state value. No signs of instability were noticed. The results of these calculations outside the immediate neighbourhood of the spreading centre will be given in another paper.

From the calculated temperature at a point (y, z) in the upper mantle, and the phase relations given in equations (5–14), the degree of partial melting and the compositions of the solid and liquid phase can be calculated at (y, z). In these calculations, it was assumed that the liquid phase at (y, z) was all the time in local equilibrium with the solid at (y, z). Phase transitions such as equations (13) and (14) are easily dealt with because the temperature remains equal to the transition temperature until the transition is completed. The extent to which such a transition has occurred is given by the ratio $R = \Delta T C_p / \Delta H$, where it is assumed that the old and new phase have the same specific heat; ΔH is the latent heat associated with the transition and ΔT is the difference between the transition temperature and the temperature calculated without taking the phase transition into account. The basalt–eclogite transition is also easily dealt with because in that case $R = (T - T_{\text{be, l}})/(T_{\text{be, u}} - T_{\text{be, l}})$ (see equation 12), where R is the fraction of basalt. Because the upper mantle liquidus is not parallel to the uppermantle solidus and the break in the solidus (equations 10*a* and *b*), the algebra to take care of melting is somewhat more involved. The melted fraction F (equation 5) should be expressed in terms of temperature, solidus and liquidus temperature for the local mantle composition by means of equations (6–11), and then with equation (2), the temperature can be calculated. Once the temperature, composition and melt distribution are known, one can evaluate heat flow, ocean bottom topography, composition and quantity of erupted liquids, and density and seisimic properties of the lithosphere. To evaluate the density of the lithosphere, use was made of the known properties of liquid basalt, solid basalt, eclogite, plagioclase peridotite, spinel peridotite, garnet peridotite and dunite (see table 3). For solid phase compositions $0 < X_s < 1$, the solid was considered to consist of a fraction X_s of solid basalt or eclogite, depending on the P and T conditions, and $(1 - X_s)$ peridotite with plagioclase, spinel or garnet depending on the P, T conditions. When $X_s > 1$, the solid was considered to consist of a fraction $1/X_s$ of peridotite with plagioclase, spinel or garnet, depending on P and T, and a fraction $(X_s - 1)/X_s$ of dunite. When $X_s < 0$, the solid was taken to be eclogite or solid basalt, depending on P and T.

TABLE 3. MATERIAL PROPERTIES OF LITHOSPHERIC MATERIALS

	density / 10^5 K^{-1}	thermal expansion / 10^{-5} K^{-1}	compressibility / bar^{-1}
basalt liquid	2.60	4	6.51
basalt solid	2.96	3.2	1.2
eclogite	3.55	3	0.525
peridotite with plagioclase	3.30	3.5	0.58
peridotite with spinel	3.33	3.5	0.58
peridotite with garnet	3.36	3.5	0.58
dunite	3.31	3.5	0.79

4. RESULTS AND DISCUSSION

First the calculated temperature field is given. This information is needed to understand properly the partial melt distribution which is discussed subsequently. Next the composition and quantity of the erupted liquids at the ridge axis are treated. Finally the density field in the axial zone is given.

4.1. *Temperature field in the upper mantle below the ridge crest*

The model calculation given here distinguishes itself from other published calculations in that heat transfer by the moving liquid, partial melting and solidification in the upper mantle are taken into account. The results of the calculations are given in figure 2; they are similar to those published previously (Bottinga & Allègre 1976). One small difference between the present and previous calculation is the horizontal boundary condition at $z = 6$ in the axial zone. Previously it was assumed that sea water penetrated the lithosphere to $z = 6$ over a width of 30 km ($0 \leqslant y \leqslant 30$); now we have taken a width of 12 km ($0 \leqslant y \leqslant 12$), causing a uniform temperature of 400 °C at this level. Seawater penetration has been intensively investigated by Lister (1974); however, it is still uncertain to which depth seawater can penetrate the lithosphere and what thermal consequences this phenomenon has. We have taken a temperature at $z = 6$ km of 400 °C, because this is suggested by the metamorphism observed in ophiolites (Spooner & Fyfe 1973); a similar value was deduced by Lewis & Snydsman (1976).

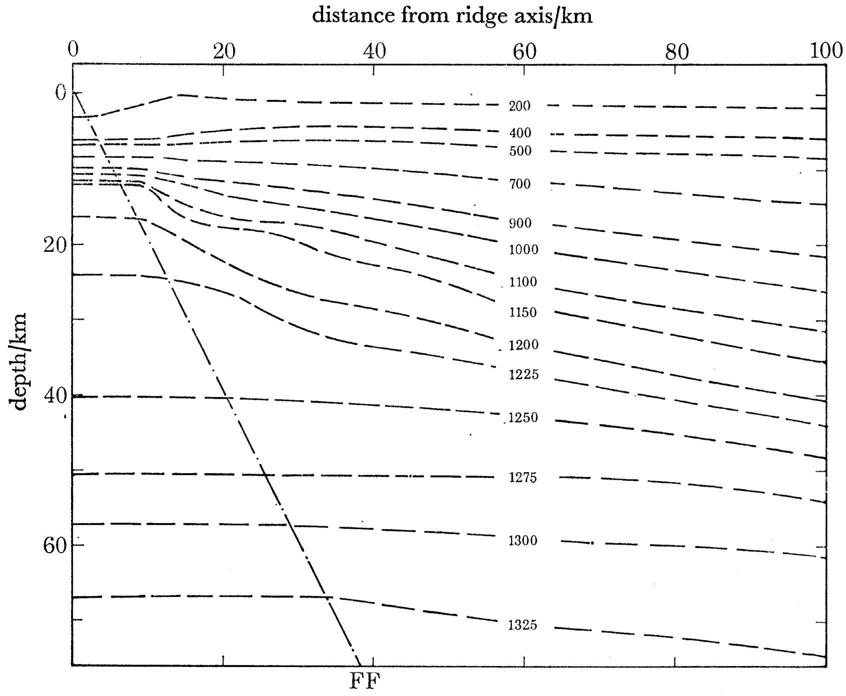

Figure 2. Isotherms for the upper mantle in the axial zone of a spreading centre. Depth is with respect to the top of layer 2. The line FF corresponds to the line B–A-2, figure 1. Half spreading rate is 1 cm/a.

This boundary condition is of no importance for the temperature in the region in the lithosphere where partial melting occurs, but because of uncertainty in this boundary condition, temperatures for depths below ocean bottom of less than 10 km and at distances less than 30 km from the ridge axis, in figure 2, should not be taken too seriously. Another reason why in this region our temperatures may be in error is that the existence of possible magma chambers in the crust at the ridge axis (Kusznir & Bott 1976) has been ignored. Further the possibility that, on a small time scale, spreading may be discontinuous (Bottinga & Allègre, 1976) will add to the uncertainty for instantaneous temperatures in this region. The grid size of 6 km which we have used in this calculation is of course inadequate to calculate precise temperatures for the oceanic crust.

The isotherm plot (figure 2) shows the influence of the flow field on the shape of the isotherms, in particular at depths of less than 40 km. The somewhat irregular features of the isotherms in the depth interval 10–30 km and up to 30 km away from the ridge axis are a result of heat transport by the mobile liquid phase and the liberation of the latent heat when this mobile liquid freezes.

The measured temperature gradients on Iceland (Palmason 1967) and São Miguel, Azores (Ade-Hall *et al.* 1974), are in agreement with the temperature distribution of figure 2. The magneto-tellurically inferred temperature and temperature gradient underneath Iceland (Hermance & Grillot 1974) are also in agreement with the results given in figure 2. Steinmetz, Whitmarsh & Moreira (1977) observed a shallow submoho zone with a V_p inversion, at 40 km away from the axis of the Mid-Atlantic Ridge a little bit north of the Azores. These authors interpreted this inversion to be due to the local presence of hydrated silicates. The temperatures implied by this interpretation are in agreement with those given in figure 2.

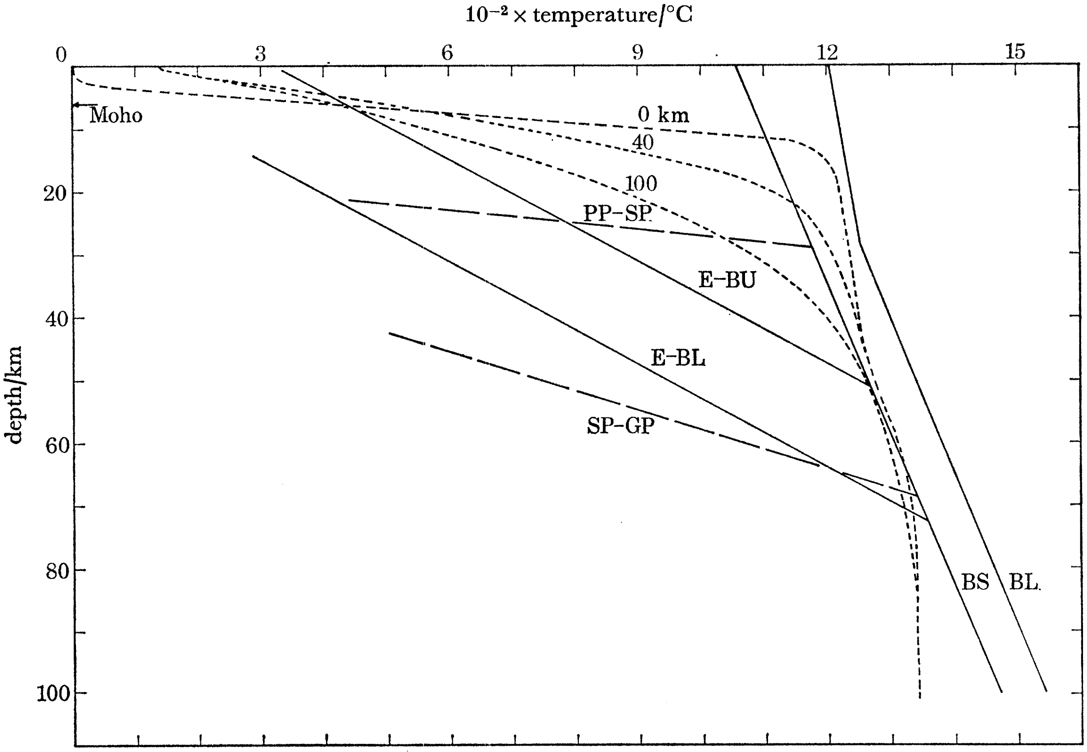

FIGURE 3. Variation of temperature with depth in the upper mantle at the ridge axis (0 km) and at 40 and 100 km from the ridge axis. Depth is relative to the top of layer 2. Also are given the curves. BL, basalt liquidus; BS, basalt solidus; E–BU, upper boundary of the transition region for the basalt–eclogite transition; E–BL, lower boundary of the transition region for the basalt–eclogite transition; PP–SP, transition plagioclase peridotite–spinel peridotite; SP–GP, transition spinel peridotite–garnet peridotite. The sources of information for these curves are mentioned in the text. Half spreading rate is 1 cm/a.

In figure 3 we have plotted the temperature distribution underneath the ridge axis, at 40 and 100 km away from the ridge axis. Also are plotted the phase relations given by equations 6–9 and 12–14. For the temperature distribution underneath the ridge axis one notices that at depths in excess of 68 km the temperature variation with depth is adiabatic (0.42 °C/km). Between 51 and 68 km depth, the basaltic component in the upwelling asthenospheric material undergoes the basalt–eclogite transition; this causes an inflection in the *P–T* path. At about 65 km depth the anhydrous solidus temperature of the upwelling asthenospheric material is reached and partial melting starts, with a latent heat adjusted to take into account the effect of the basalt–eclogite transition. At 51 km depth the latent heat of fusion is now 100 cal g^{-1} and the degree of partial melting becomes important enough to have also heat transfer by the mobile liquid phase. The result is that the temperature variation of about 2.8 °C per km in the region 51–68 km depth changes to 0.6 °C km^{-1} for the depth interval 25–50 km. At depths smaller than 30 km the liquid phase is presumed to be no longer in local equilibrium with the surrounding solid and is assumed to escape rapidly to the surface via a system of faults caused by the diverging movement of the plates in the axial zone of the ridge.

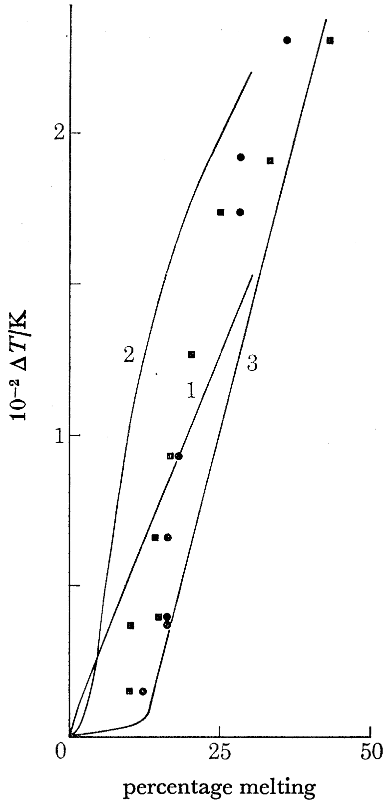

FIGURE 4. Percentage melting of a peridotite versus temperature in excess of the solidus temperature at $P = 1$ atm. Data are from Scarfe *et al.* (1972). ●, Garnet peridotite; ■, spinel peridotite; 1, Ringwood (1975); 2, Green (1971); 3, this work, equation 5.

4.2. *Partial melting*

The two aspects to be discussed are the degree and areal extent of partial melting. To calculate the extent of partial melting we have used equation (5) for the composition given in table 1, column 1, against ΔT, the difference between the actual temperature and the solidus temperature. This plot is in reasonable agreement with experimental results reported by Scarfe, Paul & Harris (1972). Also are given estimations by Ringwood (1975) and Green (1971) for pyrolite; as far as we are aware, the data on which these estimations are based have not been published. The experimental determination of the degree of melting is very difficult, in particular for small degrees of melting ($< 10\,\%$), see for instance Cawthorn *et al.* (1973). Our calculated curve (figure 4) is in qualitative agreement with a schematic curve given by

O'Hara (1968). The initial rapid increase in melted fraction can be interpreted as being due to the disappearance of feldspar which has a small melting interval for a composition of 85% peridotite (KA 64–16 (Ito & Kennedy 1968)) and 15% basalt (NM5 (Ito & Kennedy 1968)). Such a composition corresponds to the chemical composition given in table 1, column 1.

In figure 5 we give the melt distribution in the axial region of a spreading ridge. This figure is different from the one published by Bottinga & Allègre (1976) mainly because of a programming error which did not have any other consequences. To be noted is that the melt

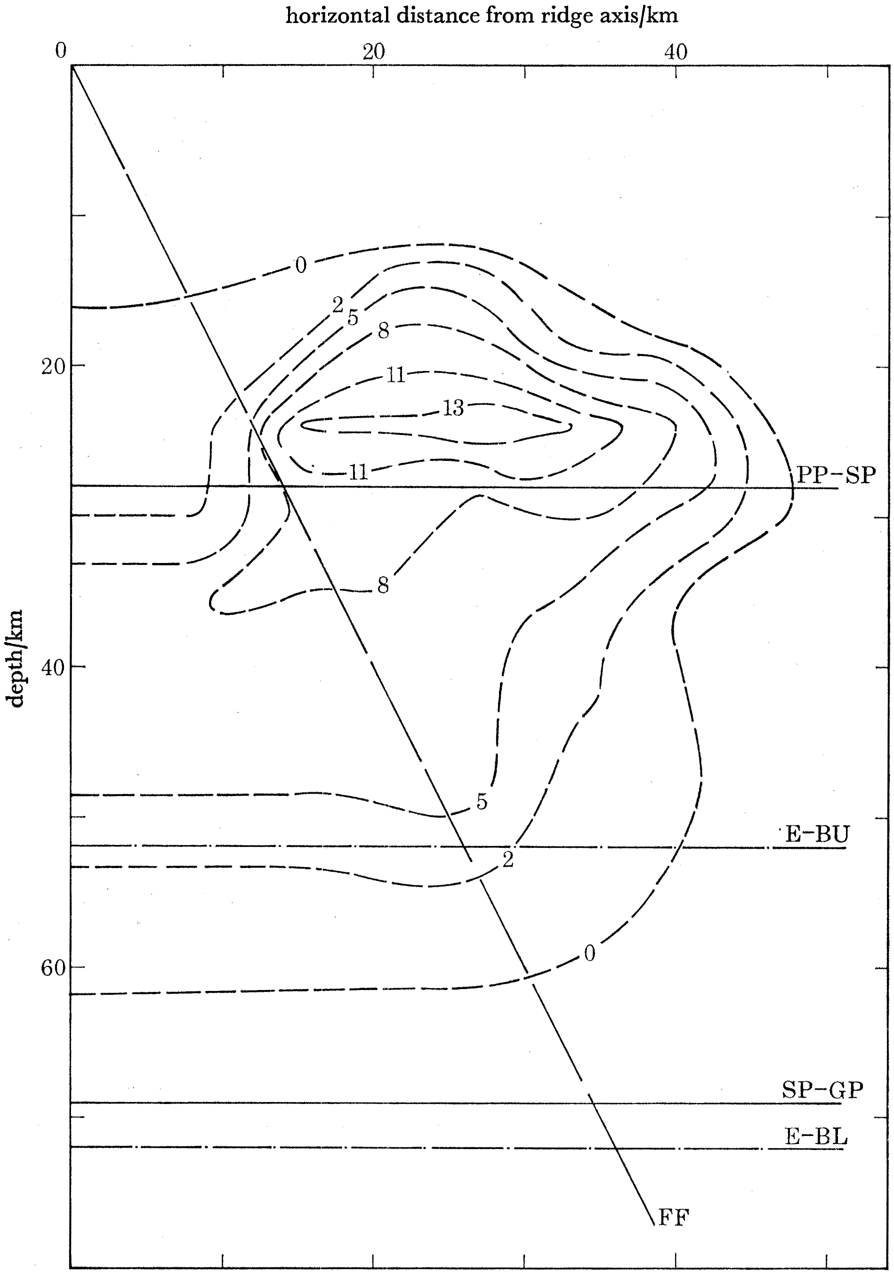

Figure 5. Partial melt distribution in the upper mantle below the ridge crest. The contours are marked by indicated percentages. The letters E–BU, E–BL, PP–SP and SP–GP have the same significance as in figure 3. The line FF corresponds to model B–A–2 (figure 1). Depth is with respect to the top of layer 2. Half spreading rate is 1 cm/a.

fraction in the upper mantle is always small: the maximum for the case we have calculated is 15% and occurs about 27 km from the ridge axis at a depth between 20 and 30 km below sea bottom. This maximum is off ridge axis because it is assumed that in an axial zone with a half width of 12 km, i.e. about the half width of the central rift valley of the mid-Atlantic Ridge (Needham & Francheteau 1974), liquid escapes from the uppermantle to erupt at the ridge axis. That indeed the largest melt concentrations are found off the ridge axis is suggested by the seismic observations of Ruegg (1975) in the Djibouti region and the analyses of the regional variation of the Poisson ratio for the same area by Vincent (1976). The liquid in the uppermantle, outside the central zone with half width of 12 km, is trapped just below Moho or may escape via fracture zones, giving rise to fracture zone volcanism.

The region where anhydrous partial melting occurs as indicated in figure 5, coincides with a region characterized by reduced shearwave velocities as determined by Jacoby & Girardin (1977) from Rayleigh wave dispersion data. The very low Q area underneath the mid-Atlantic ridge deduced by Solomon (1973) is in agreement with the partially melted zone in figure 5. This melt enriched zone should not be confused with the well known low velocity zone, because its vertical extent is rather limited as shown by the body wave data of Ruegg (1975) and the surface wave data of Jacoby & Girardin (1977) and Girardin & Jacoby (1977). The thickness of this melt enriched zone is about 15 km (see figure 5), comparable with the resolution of the data of Forsyth (1975) for the 0–10 Ma age strip of the Nazca plate. This may be the reason that this important velocity inversion was not observed by Forsyth (1975). The velocity decrease deduced for this zone by Ruegg (1975) and Jacoby & Girardin (1977) are larger than the decreases associated with the conventional low velocity zone.

Gravity observations close to the ridge axis have been interpreted by McKenzie & Bowin (1976) as indicating a shallow isostatic compensation depth. If correct, this could be associated with the liquid enriched zone.

We calculate that the total amount of material being melted in the process of asthenospheric upwelling is about 20 kg s^{-1} per kilometre of ridge length, i.e. 10 kg s^{-1} at each side of the axial plane. In our model the top of layer 3 (layer 3A) and layer 2 of the oceanic crust are the products of solidified, erupted or intruded, liquids. The bottom part of layer 3 (layer 3B) is considered to be partially serpentinized ($<$ 20%) residual harzburgite. This crustal model is conform to the seismic observations made with sonobuoys (Sutton, Maynard & Hussong 1969). At the ridge axis, 8 kg of liquid comes to the surface per second and per kilometre of ridge length for a spreading velocity of 2 cm a^{-1}. This quantity of liquid is thus only 40% of the total amount of liquid produced during asthenospheric upwelling. Lupton & Craig (1975) propose that the abundance of ^{3}He observed by them in m.o.r.b. suggests that far more melt is produced in the upper mantle below the ridge crest than is erupted at the ridge crest. The quantity of liquid which comes to the surface in our model is sufficient to construct a 3 km thick layer 3A and a 1.8 km thick layer 2. This conforms to the thickness observed for these layers; for a review see Christensen & Salisbury (1975).

The composition of the liquid erupting at the ridge crest in our model has a composition very close to the tholeiite composition, i.e. in the terminology of our model $X = -0.028$. Previously we have shown that the quantity and composition of such liquids depends only very weakly on the ascent velocity of the asthenospheric material, provided that this is larger than 1 cm a^{-1} (Allègre & Bottinga 1974; Bottinga 1974). The liquid arriving at the crest of the ridge is produced by somewhat less than 20% partial melting in our model. Unfortunately the major element composition of m.o.r.b. does not tell us directly how much partial melting occurs in the upper mantle. This is because we do not know precisely the composition of upwelling athenospheric material, the content of table 1 is mainly based on educated guesswork, and it is also sure that the m.o.r.b. composition is not just the simple product of partial fusion. These points have been extensively discussed by O'Hara (1968) and Bottinga & Allègre (1976),

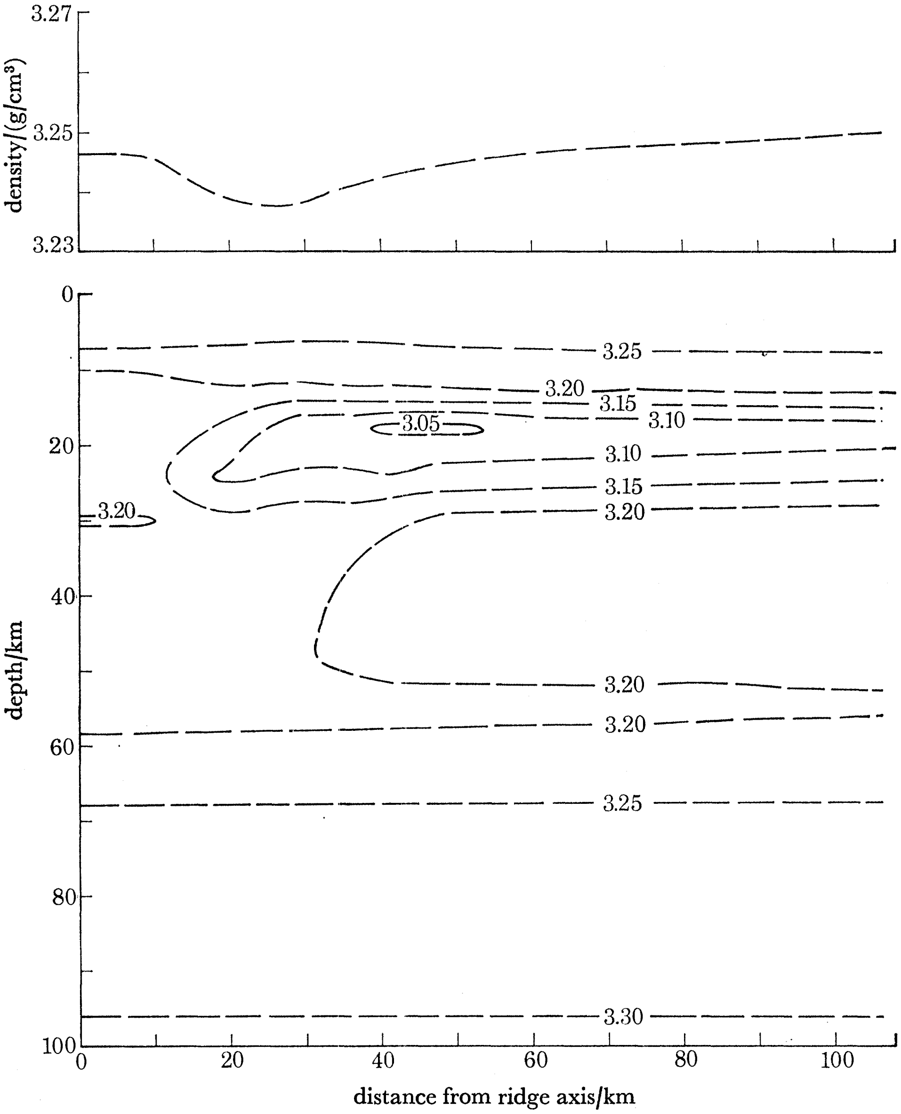

FIGURE 6. Density of the upper mantle below the ridge crest. Top diagram gives average density for the top 120 km of the mantle and how this varies with distance from the ridge axis. The bottom diagram shows density distribution in the upper mantle. Depth is with respect to the top of layer 2. Half spreading rate is 1 cm/a.

but recent developments in trace element geochemistry make it possible to obtain an idea of the degree of partial fusion needed to produce m.o.r.b. (Joron, Bougalt, Treuil & Allègre 1976; Treuil & Varet 1973). For the rocks dredged in the Famous zone, just south of the Azores in the rift valley of the Mid-Atlantic Ridge, an 8–20 % partial fusion can be calculated (Joron *et al.* 1976). We refer the reader to the papers by Allègre *et al.* (1977) and Minster, Minster, Treuil & Allègre (1977) for a rigorous discussion on the usage of trace element geochemistry in the determination of the evolution of volcanic rocks. Our calculated degree of partial fusion of somewhat less than 20 % is in agreement with this observation. The degree of partial melting is simply calculated from the total amount of melt produced by a given quantity of solid rising up from the asthenosphere in the axial plane of the ridge. Attention is drawn to the fact that the maximum amount of liquid occurring locally in the subridge uppermantle is less than degree of partial melting. This is because our system is an open system.

A comparison of figures 3 and 5 indicates that nearly all of the subridge partial melting takes place in a region where spinel–peridotite is stable in our model. This agrees with the trace element geochemistry of m.o.r.b. (Frey & Green 1974; Allègre *et al.* 1973).

Second order variations in the chemical composition of mid-oceanic ridge basalts have been reported repeatedly in the literature (Christensen *et al.* 1973; Joron *et al.* 1976). In our model, chemical equilibrium between residual solid and melt is attained only locally, i.e. the liquid erupted at the surface is not supposed to be in equilibrium with all of the solid phase in the region between 25 and 68 km where it is produced. Also it is possible that during its ascent the liquid produced at different depths does not mix completely enough to produce at the surface a continuous stream of homogeneous basalt. Moreover, the plate velocity may not be constant on a time scale small in comparison with the ocean bottom magnetic anomaly time scale (Bottinga & Allègre 1976) and this means that there could be velocity variations in the upwelling with as a result chemical variations in the erupting basalts (Allègre & Bottinga 1974).

In figure 6 we give the average density in the top 120 km of the sub-ridge uppermantle and also the density distribution in this part of the Earth as a function of distance from the axial plane of the ridge. This information is needed if one wishes to analyse the dynamics of a spreading centre (see, for instance, Lachenbruch 1976). As to be expected, significant density variations occur in this region in our model. These density variations do not explain all the aspects of gravity anomalies associated with spreading ridges. As remarked by Talwani (1970) and Lambeck (1972) part of the gravity anomaly associated with a spreading centre must originate at depth of more than 100 km.

5. General remarks

The topography of the ocean bottom close to the ridge axis ($0 \leqslant y \leqslant 100$ km) could be a very important constraint on the theoretical estimates of partial melting in the upper mantle. However, uncertainty on the depth of the level of compensation, as illustrated by the estimates of McKenzie & Bowin (1976) and Parsons & Sclater (1977), make a demonstration that the observed topography and calculated topography are in agreement, but not very convincingly. We do not know a physical reason why the interior of the Earth beneath the oceans should be uniform gravitationally at depths greater than the steady state plate thickness, as demanded by the Parsons & Sclater model. In Benioff zones, the sinking lithosphere can be traced down to several hundred kilometres depth; hence it is reasonable to assume that part of the upwelling material underneath the ridge crest also comes from a depth considerably greater than the steady state plate thickness. Anyhow, the model presented in this paper reproduces also the topography as given by Parsons & Sclater (1977), with a compensation level at 126 km below sea bottom, as is the case for the Parsons & Sclater model.

Unfortunately the seismic information we have for the upper mantle below spreading ridges does not allow a quantitative understanding of what is going on. The reason for this is twofold: on the one hand the theory which deals with the acoustic properties of partially melted materials (Walsh 1969) does not seem to be applicable (see Bottinga & Allègre 1976) and on the other hand the seismic observations show apparent contradictions. Hart & Press (1973) reported that shear wave velocities in the lithosphere below the Mid-Atlantic Ridge were larger than those underneath the flanks of the ridge. Woollard (1975) and Neprochnov & Rykunov (1970) published compressional wave velocities in excess of 9 km s^{-1} for the upper mantle below the actively spreading ridges. In contradiction of this, however, we have the observations of Molnar & Olivier (1969), Solomon (1973), Solomon & Julian (1973), Girardin & Jacoby (1977) and Forsyth (1975) which show that the subridge uppermantle is characterized by reduced acoustic properties. We do not know of any reported experimental data on the measurement of Q, V_p and V_s in partially melted peridotite. The often quoted experiments on the acoustic properties of the salt-water system by Anderson & Spetzler (1970), are very interesting but a poor substitute for a partly melted peridotite. In a peridotite early melting will affect mainly the clinopyroxene and the aluminous phase (see Ito & Kennedy 1968) while eutectic melting in the NaCl–water system will probably cause the formation of a fluid film around all crystals. An additional complicating factor is the occurrence of acoustic anisotropy even close to the ridge axis (Keen & Tramontini 1970; Snydsman, Lewis & McClain 1975) which is difficult to model.

In the model used in this paper, there are some parameters which were to a certain extent arbitrarily fixed. This is true in particular for the adopted flow field, the upper mantle composition and the region of the upper mantle from which liquid drained, to be erupted at the ridge crest. Our choice of flow field was based on the following reasons: (*a*) heat flow in the region $0 \leqslant y \leqslant 100$ km; (*b*) topography, as affected by the presence of partial melt in the upper mantle also in the region $0 \leqslant y \leqslant 100$ km; (*c*) vertical bulk velocities in the upper mantle underneath the ridge axis should be reasonable; (*d*) the width of the partial melting zone should not be excessive. Our choice of composition was guided by estimates made by Ringwood (1975), Carter (1970) (see table 1), by the known seismic properties of the upper mantle and by the degree of partial melting needed to make m.o.r.b. (see Joron *et al.* 1976). Our choice for the width of the region underneath the ridge crest drained of its partial melt to produce layers 2 and 3A, was only based on the need to have sufficient liquid and the right composition at the ridge axis.

The partial melting model presented here has as a consequence that the lithosphere away from the ridge axis is not only mineralogically zoned but also chemically (Bottinga 1974; Bottinga & Allègre 1976). This zonation affects the sea bottom topography as well as the acoustic properties of the lithosphere away from the ridge axis. In a future contribution these aspects are to be discussed and shown to be in agreement with observations. Our model is of course too simple to be petrologically very meaningful. However, from an energetic point of view, we believe it may not be too bad, but it should be obvious that far more data are needed on the latent heat of fusion of rocks and minerals and the solid–liquid relations of even a very simplified representative system of the uppermantle, as the system C_2O–MgO–Al_2O_3–SiO_2, before significant progress can be made along the lines indicated in this paper.

We should like to acknowledge the various friendly discussions we have had on the subject of partial melting with our colleague Nobu Shimizu.

REFERENCES (Bottinga & Allègre)

Adams, L. H. & Cohen, L. H. 1966 *Am. J. Sci.* **264**, 543–561.

Ade-Hall, J. M., Aumento, F., Muecke, G. K., McDonald, A., Hyndman, R. D., Quinto, J., Opdyke, N. & Lowrie, W. 1974 *Eos* **55**, 454 (abstract).

Allègre, C. J. & Bottinga, Y. 1974 *Nature, Lond.* **252**, 31–32.

Allègre, C. J., Montigny, R. & Bottinga, Y. 1973 *Bull. Soc. géol. Fr.* **15**, 461–478.

Allègre, C. J., Treuil, M., Minster, J. F., Minster, B. & Albarède, F. 1976 *Contr. Miner. Petrol.* **60**, 57–75.

Anderson, A. T. 1975 *Rev. Geophys. Space Phys.* **13**, 37–56.

Anderson, D. L. & Spetzler, H. 1970 *Phys. Earth planet. Inter.* **4**, 62–64.

Bacon, C. R. 1975 *Abstract, Geol. Soc. Am., Ann. Mtg Salt Lake City, Utah*, pp. 983–984.

Bamford, D. 1973 *Z. Geophys.* **39**, 907–927.

Barin, I. & Knacke, O. 1973 *Thermodynamical properties of inorganic substances*. Berlin: Springer-Verlag.

Beswick, A. E. 1976 *Geochim. cosmochim. Acta* **40**, 1167–1184.

Biggar, G. M. & O'Hara, M. J. 1969 *Progress in experimental petrology*, 1st rept., pp. 86–96. N.E.R.C.

Bottinga, Y. 1974 *Tectonophysics* **21**, 15–38.

Bottinga, Y. & Allègre, C. J. 1973 *Tectonophysics* **18**, 1–17.

Bottinga, Y. & Allègre, C. J. 1976 *Tectonophysics* **32**, 9–59.

Bottinga, Y., Steinmetz, L. & Allègre, C. J. 1976 *Bull. Soc. géol. Fr.* **18**, 941–947.

Bottinga, Y. & Weill, D. F. 1970 *Am. J. Sci.* **269**, 169–182.

Bottinga, Y. & Weill, D. F. 1972 *Am. J. Sci.* **272**, 438–475.

Boudier, F. 1976 Thèse de Doctorat d'État. Université de Nantes.

Boudier, F. & Nicolas, A. 1972 *Bull. Suisse miner. petrogr.* **52**, 39–56.

Boyd, F. R. 1964 *Science, N.Y.* **145**, 13–20.

Boyd, F. R. & England, J. R. 1963 *J. geophys. Res.* **68**, 311–323.

Bradley, R. S. 1962 *Am. J. Sci.* **260**, 550–554.

Burnham, C. W. & Davis, N. F. 1974 *Am. J. Sci.* **274**, 902–940.

Carmichael, I. S. E., Turner, F. J. & Verhoogen, J. 1974 *Igneous petrology*, 739 pages. New York: McGraw-Hill.

Carter, J. L. 1970 *Bull. geol. Soc. Am.* **81**, 2021–2034.

Cawthorn, R. G., Ford, C. E., Biggar, G. M., Bavo, M. S., Clarke, D. B. 1973 *Earth planet. Sci. Lett.* **21**, 1–5.

Christensen, N. I., Frey, F. A., MacDougal, D., Melson, W. G., Peterson, M. N. A., Thompson, G. & Watkins, N. D. 1973 *Eos* **54**, 972–981.

Christensen, N. I. & Salisbury, M. H. 1975 *Rev. Geophys. Space Phys.* **13**, 57–86.

Cohen, L. H., Ito, K. & Kennedy, G. C. 1967 *Am. J. Sci.* **265**, 475–518.

Craig, H., Boato, G. & White, D. E. 1956 *Proc. 2nd Conf. Nucl. Processes, Geol. Settings.* Publ. 400, NAS–NRC.

Craig, H. & Lupton, J. E. 1976 *Earth planet. Sci. Lett.* **31**, 369–385.

Crough, S. T. 1975 *Nature, Lond.* **256**, 388–390.

Davies, H. L. 1971 Bureau of Mineral resources, Geology and Geophysics, Dept. of National Development, Bull. 128, Canberra, Australia, 48 pages.

De Bremaecker, J. C. 1975 *Geophys. J.* **45**, 349–356.

Detrick, R. S., Williams, D. L., Mudie, J. D. & Sclater, J. G. 1974 *Geophys. J.* **38**, 627–637.

Dickey, J. S. Jr 1970 *Mineral. Soc. Am. Sp. Paper*, **3**, 33–49.

Ferrier, A. 1968 *C.r. hebd. Séanc. Acad. Sci., Paris* **267**, 101–103.

Ferrier, A. 1969 *C.r. hebd. Séanc. Acad. Sci., Paris* **269**, 951–954.

Forsyth, D. W. 1975 *Geophys. J.* **43**, 103–162.

Forsyth, D. W. & Press, F. 1971 *J. geophys. Res.* **76**, 7963–7979.

Franck, F. C. 1968 *Nature, Lond.* **220**, 350–352.

Frey, F. A. & Green, D. H. 1974 *Geochim. cosmochim. Acta* **38**, 1023–1060.

Fuchs, K. 1975 *Geol. Rdsch.* **64**, 700–716.

Gerlach, T. M. & Nordlie, B. E. 1975 *Am. J. Sci.* **275**, 395–410.

Giggenbach, W. F. & Le Guern, F. 1976 *Geochim. cosmochim. Acta* **40**, 25–30.

Girardin, N. & Jacoby, W. R. 1977 *Tectonophysics* (In the press.)

Green, D. H. 1964 *J. Petr.* **5**, 134–188.

Green, D. H. 1971 *Phil. Trans. R. Soc. Lond.* A **268**, 707–725.

Green, D. H. & Lieberman, R. C. 1976 *Tectonophysics* **32**, 61–92.

Green, D. H. & Ringwood, A. E. 1967 *Contr. Miner. Petr.* **15**, 103–190.

Green, D. H. & Ringwood, A. E. 1970 *Phys. Earth planet. Inter.* **3**, 359–371.

Hariya, Y. & Kennedy, G. C. 1968 *Am. J. Sci.* **266**, 193–203.

Hart, R. S. & Press, F. 1973 *J. geophys. Res.* **78**, 407–411.

Hermance, J. F. & Grillot, L. R. 1974 *Phys. Earth planet. Inter.* **8**, 1–12.

Herzberg, C. T. & Chapman, N. A. 1976 *Am. Miner.* **61**, 626–637.

Hess, H. H. 1964 *Nature, Lond.* **203**, 629–631.
Ito, K. & Kennedy, G. C. 1967 *Am. J. Sci.* **265**, 211–217.
Ito, K. & Kennedy, G. C. 1968 *Contr. Miner. Petr.* **19**, 177–211.
Jackson, E. D. & Wright, T. L. 1970 *J. Petr.* **11**, 405–430.
Jacoby, W. R. & Girardin, N. 1977 (Preprint.)
Janaf, 1971 *Thermodynamical tables*, 2nd edn, NSRDS–NBS 37. U.S. Dept. of Commerce and Nat. Bureau of Standards.
Jehl, V. 1975 Thèse de Docteur-Ingénieur, Université de Nancy I.
Joron, J. L., Bougault, H., Treuil, M. & Allègre, C. J. 1976 *Bull. Soc. géol. France* **18**, 811–818.
Juteau, T. 1974 Thèse de Doctorat d'Etat, Université de Nancy I.
Kawada, K. 1966 *Bull. Earthq. Res. Inst., Tokyo Univ.* **44**, 1071–1091.
Keen, C. & Tramontini, C. 1970 *Geophys. J.* **20**, 473–491.
Kelley, K. K. 1960 *Contribution to the data on theoretical metallurgy. XIII. High temperature heat content, heat capacity and entropy data for the elements and inorganic compounds.* Washington, D.C.: U.S. Government Printing Office.
Kelley, K. K. 1962 *U.S. Bureau of Mines, Rept. Invest.* 5901, 32 pages.
Kohlstedt, D. L., Goetze, C. & Durham, W. B. 1976 In *The physics and chemistry of minerals and rocks* (ed. R. G. J. Strens), pp. 35–50. New York: Wiley.
Kornprobst, J. 1969 *Contr. Miner. Petr.* **23**, 283–322.
Kracek, F. C. & Neuvonen, K. J. 1952 *Am. J. Sci.*, Bowen volume, 293–318.
Kubaschewski, O., Evans, E. L. & Alcock, C. B. 1967 *Metallurgical thermochemistry*, 4th ed. London: Pergamon Press.
Kushiro, I. 1964 *Carnegie Instn Wash. Yb.* **63**, 83–84.
Kushiro, I. 1972 *Am. Miner.* **57**, 1260–1271.
Kushiro, I., Satake, N. & Akimoto, S. 1975 *Earth planet. Sci. Lett.* **28**, 116–120.
Kushiro, I., Syono, Y. & Akimoto, S. 1968 *J. geophys. Res.* **73**, 6023–6029.
Kusznir, N. J. & Bott, M. H. P. 1976 *Geophys. J.* **47**, 83–95.
Lachenbruch, A. H. 1976 *J. geophys. Res.* **81**, 1883–1902.
Lambeck, K. 1972 *Geophys. J.* **30**, 37–53.
Lang, A. R. 1972 *Nature, Lond.* **238**, 98–100.
Langseth, M. G., Le Pichon, X. & Ewing, M. 1966 *J. geophys. Res.* **71**, 5321–5355.
Le Pichon, X., Francheteau, J. & Bonnin, J. 1973 *Plate tectonics.* Amsterdam: Elsevier.
Lewis, B. T. R. & Snydsman, W. E. 1976 (Preprint.)
Lindsley, D. H. 1966 *Carnegie Inst. Wash. Yb.* **65**, 226–230.
Lister, C. R. B. 1974 *Geophys. J.* **39**, 465–509.
Loubet, M. 1976 Thèse de Doctorat d'Etat, Universitè de Paris VII.
Loubet, M., Shimizu, N. & Allègre, C. J. 1975 *Contr. Miner. Petr.* **53**, 1–12.
Lupton, J. E. & Craig, H. 1975 *Earth planet. Sci. Lett.* **26**, 133–139.
MacGregor, I. D. 1974 *Am. Miner.* **59**, 110–119.
McKenzie, D. P. 1967 *J. geophys. Res.* **72**, 6261–6273.
McKenzie, D. P. & Bowin, C. 1976 *J. geophys. Res.* **81**, 1903–1915.
Minster, J. F., Minster, J. B., Treuil, M. & Allègre, C. J. 1977 *Contr. Miner. Petr.* **61**, 49–77.
Molnar, P. & Olivier, J. 1969 *J. geophys. Res.* **74**, 2648–2682.
Montigny, R. 1975 Thèse de Doctorat d'Etat, Université Paris VII.
Moore, J. G. 1970 *Contr. Miner. Petr.* **28**, 272–279.
Moore, J. G. & Schilling, J. G. 1973 *Contr. Miner. Petr.* **41**, 105–118.
Moores, E. M. 1969 *Geol. Soc. Am. Spec. Pap.* **118**, 74 pages.
Morgan, W. J. 1972 *Bull. Am. Ass. Petrol. Geol.* **56**, 203–213.
Morris, G. B., Raitt, R. W. & Shor, G. C. 1969 *J. geophys. Res.* **74**, 4300–4316.
Needham, H. D. & Francheteau, J. 1974 *Earth planet. Sci. Lett.* **22**, 29–43.
Neprochnov, Y. & Rykunov, L. N. 1970 *Dokl. Akda. Nauk SSSR* **194**, 80–82.
Newton, R. C. & Sharp, W. E. 1975 *Earth planet. Sci. Lett.* **26**, 239–244.
Nordlie, B. F. 1971 *Am. J. Sci.* **271**, 417–463.
Obata, M. 1976 *Am. Miner.* **61**, 804–816.
Oldenburg, D. W. 1975 *Geophys. J.* **43**, 425–451.
O'Hara, M. J. 1968 *Earth Sci. Rev.* **4**, 69–133.
O'Hara, M. J., Richardson, S. W. & Wilson, G. 1971 *Contr. Miner. Petr.* **32**, 48–68.
Orr, R. L. 1953 *J. Am. chem. Soc.* **75**, 528–532.
Palmason, G. 1967 *Iceland and mid-oceanic ridges* (R.I.T.), vol. 38, pp. 111–127.
Parker, R. L. & Oldenburg, D. W. 1973 *Nature, Lond.* **242**, 137–139.
Parrot, J. F. 1967 *Le cortège ophiolitique du Pinde septentrional (Grèce)*, pp. 1–114. Paris: O.R.S.T.O.M.
Parsons, B. & Sclater, J. G. 1977 *J. geophys. Res.* **82**, 803–828.
Pineau, F., Javoy, M. & Bottinga, Y. 1976 *Earth planet. Sci. Lett.* **29**, 413–421.
Pucetti, A. & Bueddemeier, R. W. 1974 *Eos* **55**, 488 (abstr.).

Richter, F. M. 1973 *J. geophys. Res.* **78**, 8735–8745.
Ringwood, A. E. 1966 *Advances in Earth science*, pp. 357–399. Cambridge, Mass: M.I.T. Press.
Ringwood, A. E. 1975 *Composition and petrology of the Earth's mantle*. New York: McGraw-Hill.
Robie, R. A. & Waldbaum, D. R. 1968 *U.S.G.S. Bull.* 1259, Washington, D.C.: U.S. Government Printing Office.
Roedder, E. 1965 *Am. Miner.* **50**, 1746–1782.
Ruegg, J. C. 1975 *Ann. géophys.* **31**, 329–360.
Scarfe, C. M., Paul, D. K. & Harris, P. G. 1972 *Neues Jb. Miner. Mh.* **10**, 469–476.
Schatz, J. F. & Simmons, G. 1972 *J. geophys. Res.* **77**, 6966–6983.
Sclater, J. G. & Francheteau, J. 1970 *Geophys. J.* **20**, 509–542.
Sheppard, S. M. F. & Epstein, S. 1970 *Earth planet. Sci. Lett.* **9**, 232–239.
Shor, G. C. Jr, Menard, H. W. & Raitt, R. W. In *The sea*, vol. 4, pp. 3–28.
Skinner, B. J. 1974 *Geol. Soc. Am. Mem.* **97**, 75–96.
Sleep, N. H. 1974 *Bull. geol. Soc. Am.* **85**, 1225–1232.
Snydsman, W. E., Lewis, B. T. R. & McClain, J. 1975 *Earth planet. Sci. Lett.* **28**, 46–50.
Solomon, S. C. 1973 *J. geophys. Res.* **78**, 6044–6059.
Solomon, S. C. & Julian, B. R. 1974 *Geophys. J.* **38**, 265–285.
Spooner, E. T. C. & Fyfe, W. S. 1973 *Contr. Miner. Petr.* **42**, 287–304.
Steinmetz, L., Whitmarsh, R. B. & Moreira, V. S. 1977 *Geophys. J.* **50**, 353–380.
Stoiber, R. E. & Jepsen, A. 1973 *Science, N.Y.* **182**, 577–578.
Sutton, G. H., Maynard, J. L. & Hussong, D. M. 1971 *Am. geophys. Un. Monogr.* **14**, 193–210.
Talwani, M. 1970 In *The sea*, vol. 4, pp. 251–297.
Thorarinson, S. 1970 *Bull. volcan.* **33**, 910–927.
Treuil, M. & Varet, J. 1973 *Bull. Soc. géol. Fr.* **15**, 500–506.
Turcotte, D. L. & Oxburgh, E. R. 1972 *Rev. Fluid Mech.* **4**, 33–68.
Vincent, C. M. 1976 *Rapport D.E.A. Géophysique Interne*, Université Paris VI.
Waldbaum, D. R. 1968 *Contr. Miner. Petr.* **17**, 71–77.
Walsh, J. B. 1969 *J. geophys. Res.* **74**, 4333–4337.
White, R. W. 1966 *Contr. Miner. Petr.* **12**, 245–314.
Williams, D. L. & von Herzen, R. P. 1974 *Geology* **2**, 327–328.
Williams, D. L., von Herzen, R. P., Sclater, J. G. & Anderson, R. N. 1974 *Geophys. J.* **38**, 587–608.
Woollard, G. P. 1975 *Rev. Geophys. Space Phys.* **13**, 87–137.
Wyllie, P. J. 1971 *The dynamic Earth*. New York: Wiley.

Discussion

R. N. THOMPSON (*Department of Geology, Imperial College, London SW7 2ZA*). The authors' thermal–petrological model gives a postulated depth interval for basic magma production beneath mid-oceanic ridges and Iceland which accords well with the range of silica saturation observed in the lavas of these regions. The choice in this model of a basalt with a 1 atm liquidus just above 1200 °C to represent the liquid produced by partial mantle fusion seems to me, however, to be open to the following doubt. Tilley, Thompson & Lovenbury (1972) did not determine the composition of liquidus olivine in the Mid-Atlantic Ridge olivine tholeiite (T89) with a 1 atm liquidus of 1212 °C studied by them. This may nevertheless be calculated to be Fo_{81} by using the widely accepted value of 0.33 for the distribution coefficient of FeO and MgO between olivine and liquid (Fe_2O_3 in T89 is taken as the analysed figure of 1.55 %). Olivine Fo_{81} is appreciably more Fe-rich than the value of Fo_{83} deduced by the authors of several recent geophysical and petrological studies to be the olivine composition in 'fertile' upper mantle, such as rises beneath spreading ridges. It seems probable, therefore, that a Fo_{81} basalt would have undergone some fractional crystallization between genesis and eruption.

Recent studies of ocean-floor basalts, particularly samples collected during the Deep Sea Drilling Project, have demonstrated that basalts containing olivine phenocrysts Fo_{89-91} have a wide sporadic distribution along spreading axes. The olivine in these lavas overlaps the compositional range of olivine in postulated samples of basalt-depleted lithospheric sub-oceanic upper mantle, found as peridotite xenoliths in the ejecta of some ocean-island volcanoes and as the lower parts of ophiolite complexes. If the foregoing constraints are correct, it is apparent that a thermal-petrological model for magma production at spreading ridges should allow either for the production of melts in equilibrium with olivine ranging from Fo_{84} (incipient fusion) to Fo_{91} (maximum fusion) or for the latter alone, postulating fractional crystallization to derive the less-magnesian lavas. The estimated 1 atm liquidus of a Fo_{91} magma is approximately 1350 °C, the exact value depending *inter alia* upon the postulated abundance of chromite microphenocrysts.

Reference

Tilley, C. E., Thompson, R. N. & Lovenbury, P. A. 1972 *Geol. J.* **8**, 59–64.